Volume 5 | Number 16 | 28 April 2017 | Pages 3859–4086

Journal of Materials Chemistry C

Materials for optical, magnetic and electronic devices

rsc.li/materials-c

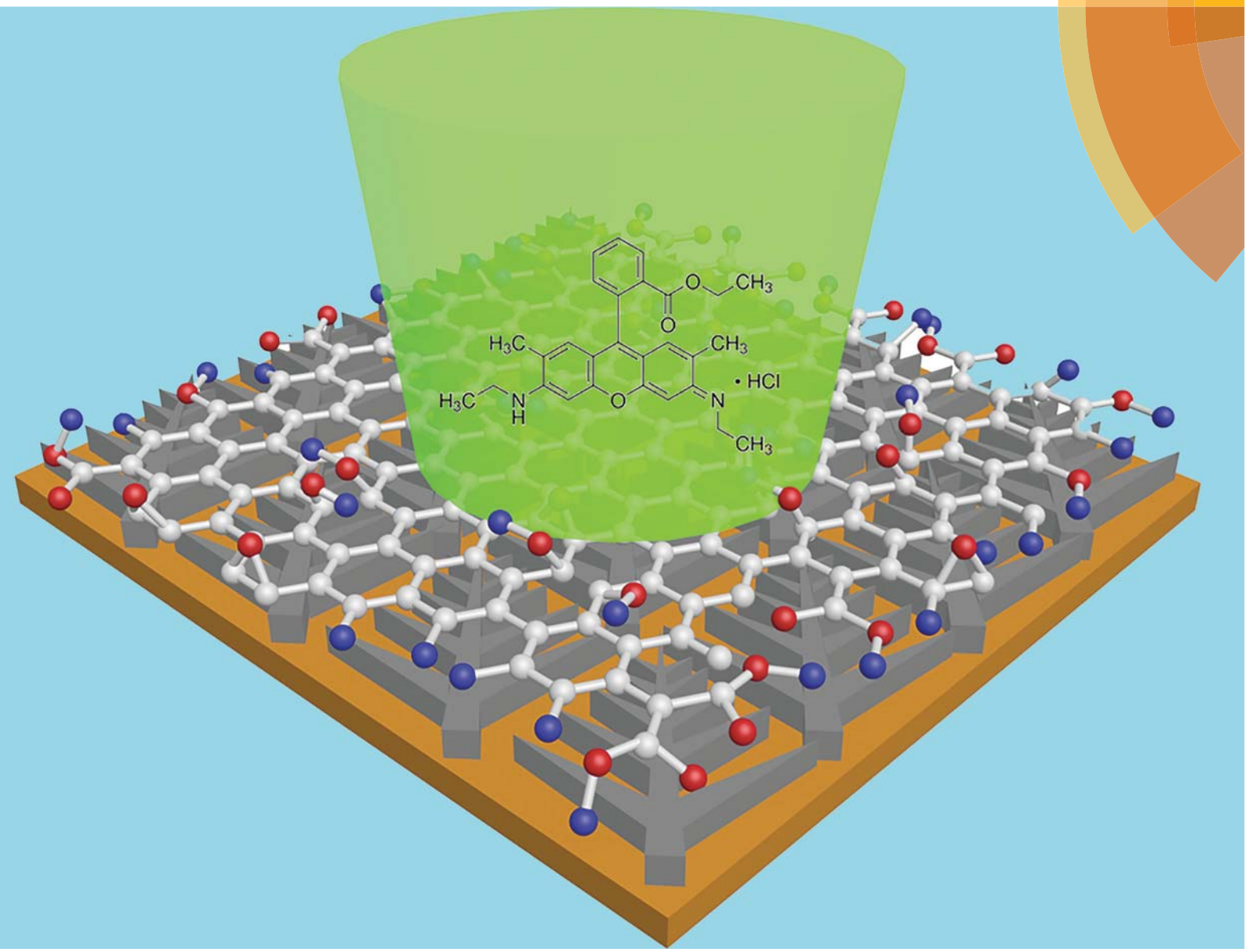

ISSN 2050-7526

ROYAL SOCIETY OF CHEMISTRY

PAPER

Yan Jun Liu, Shouzhen Jiang *et al.*

Graphene oxide-decorated silver dendrites for high-performance surface-enhanced Raman scattering applications

Journal of
Materials Chemistry C

PAPER

Cite this: J. Mater. Chem. C, 2017, 5, 3908

Graphene oxide-decorated silver dendrites for high-performance surface-enhanced Raman scattering applications†

Litao Hu,[ab] Yan Jun Liu,*[a] Yanshun Han,[c] Peixi Chen,[b] Chao Zhang,[b] Chonghui Li,[b] Zhengyi Lu,[b] Dan Luo[a] and Shouzhen Jiang*[b]

Received 23rd January 2017,
Accepted 24th March 2017

DOI: 10.1039/c7tc00381a

rsc.li/materials-c

We demonstrate graphene oxide (GO)-decorated Ag dendritic nanostructures on a copper substrate for surface enhanced Raman scattering (SERS) applications. The Ag dendrites (AgD) were synthesized through a facile and low-cost galvanic replacement reaction of Ag nitrate solution and copper foils. The AgD/Cu was further decorated with GO by a dip-coating method. The GO-decorated AgD exhibited a much higher SERS activity in terms of sensitivity, signal-to-noise ratio and stability compared with non-decorated AgD, indicating that the GO/AgD/Cu substrates could be potentially useful for highly sensitive molecule detecting applications.

1. Introduction

Nowadays, our modern society presents an ever-increasing need in technological advances for applications such as life care, environmental monitoring, food safety, and security. Surface-enhanced Raman scattering (SERS) spectroscopy appears as a highly promising analytical tool in this direction due to its unprecedented capability with label-free, highly-sensitive, surface-selective, and multiplexed analysis.[1–3] As is known, the SERS signals are heavily dependent on the substrates. Various types of substrates have been designed and developed to enhance the SERS sensitivity for practical applications.[4–12] Among them, noble metal-based substrates have demonstrated superior SERS activity since tremendous hot spots can be created in noble metallic nanostructures, which provide an extremely strong electromagnetic field around the hot spots due to the excitation of surface plasmons.[10–12] This plasmon-induced field enhancement underpins SERS for the highly-sensitive detection and analyses of different analytes.

Thus far, various types of SERS substrates based on noble metallic nanostructures have been heavily investigated.[13–16] The determining factors that govern the final success of a SERS sensor ultimately lie in the facile, low-cost substrate fabrication and the high-performance SERS activity. Among those noble metals, Ag stands out given the fact that Ag nanostructures not only have an easy fabrication/synthesis but also demonstrate superior SERS activity. Ag-based SERS substrates can be fabricated in many different ways, such as electrochemical deposition,[17] chemical vapor deposition (CVD),[18] micro/nano-fabrication,[19] and chemical synthesis.[20] Various morphologies, such as nanoparticles,[21] nanocubes,[22] nanoplates,[23] and nanostars,[24] have been extensively tested as SERS substrates. Compared with other nanostructures, the Ag dendrite—a hierarchical nanostructure that consists of multi-level branches—has attracted particular interest due to its unique optical, electrical and catalytic characteristics.[25,26] Though the growth mechanism of dendritic silver nanostructures is still under debate, it has been widely accepted that such nanostructures result from two combined growth mechanisms: Ostwald ripening (OR) and oriented attachment (OA). Recently, we have proposed and discussed the growth mechanism in detail based on the morphological evolution.[27] Such complex nanostructures can provide a huge amount of "hot spots" at the end of branches or the junctions of adjacent Ag branches,[28] which are particularly favorable for SERS detection.[29,30] Ag dendrites have also been investigated for other potential applications such as biochemical sensors,[31,32] catalysis,[33] and superhydrophobic surfaces.[34]

Compared to Au, whose plasmonic resonance is damped by the interband transitions, Ag is thought to be an ideal Raman enhancing material in terms of high efficacy and cost-effectiveness.[30,35] However, Ag suffers from its tendency to oxidation, posing serious limitations for its use as a reliable, reproducible long-term SERS substrate. Moreover, spurious signals induced by the Ag nanostructure itself may also cause additional fluctuation, reducing the signal-to-noise ratio of SERS measurement.

[a] Department of Electrical and Electronic Engineering, Southern University of Science and Technology, Shenzhen 518055, China. E-mail: yjliu@sustc.edu.cn
[b] School of Physics and Electronics, Shandong Normal University, Jinan 250014, China. E-mail: jiang_sz@126.com
[c] Qilu Institute of Technology, Jinan 250200, China

† Electronic supplementary information (ESI) available. See DOI: 10.1039/c7tc00381a

Graphene, as a two-dimensional nanomaterial reported since 2004,[36] has also demonstrated promising potential for SERS sensing applications since because it could adsorb and concentrate the target molecules and magnify the SERS signal.[37,38] As one of the most important graphene derivatives, graphene oxide (GO) has superior bio-compatibility and chemical stability due to a large quantity of hydrophilic oxygenated functional groups,[39,40] which is much more significant for the selective adsorption of molecules and stable SERS signals with perfect bio-compatibility, homogeneity and chemical stability.

Given the aforementioned reasons, marriage of Ag nanostructures and graphene or its derivatives has emerged as an excellent candidate for SERS materials and gained increasing attention in the past few years.[41–53] For instance, Ag-decorated GO or GO-covered Ag substrates have been used for detecting aromatic molecules by exploiting the strong interaction between these molecules with the graphene surface.[45–48] Thus far, previous studies have focused mainly on coating Ag nanoparticles on a planar surface. GO-decorated Ag dendritic nanostructures have been rarely studied. The hierarchical structure of the GO-decorated Ag dendrite could make it an excellent candidate material for SERS, enabling even better sensitivity and stability compared to other GO–Ag structures.

In this paper, we investigate the GO-decorated Ag dendritic nanostructures on a copper substrate for SERS applications. Compared with the AgD/Cu substrate, the GO/AgD/Cu substrate shows much better performance in terms of sensitivity, signal-to-noise ratio, uniformity, and stability. The minimum detected concentration from the GO/AgD/Cu substrate of R6G can reach 10^{-11} M, which is one order of magnitude lower than that from AgD/Cu substrate. Experimental results also show that GO decoration can effectively prevent the oxidation of Ag dendrites and hence enable the long-term stability of the SERS signal.

2. Experimental

Fig. 1 shows the schematic preparation processes of the GO/AgD/Cu substrate. The Cu foils were cut into pieces with the size of 1 cm × 1.5 cm and washed subsequently with acetone, ethanol and deionized (DI) water to remove any organic impurities. To obtain fresh Cu surfaces, the cleaned Cu foils were immersed in 1% by weight diluted sulfuric acid for 3 min to remove surface oxides and then thoroughly rinsed with DI water. The pretreated Cu foils were immersed into an aqueous solution of $AgNO_3$ with a concentration of 10 mM for 5 min and the galvanic replacement reaction took place. The Ag ions from the solution were continuously reduced by Cu atoms through electron transfer from the underlying Cu atoms, and the reduced Ag atoms were then deposited on the Cu surface. As the reaction continued, Ag dendritic nanostructures gradually formed on the Cu foils. Next, GO dispersion with the concentration of 0.4 mg ml^{-1} was immediately spin-coated on the AgD/Cu substrate at 2000 rpm for 45 s, forming the GO/AgD/Cu substrate.

The morphologies of the AgD/Cu and GO/AgD/Cu substrates were observed under a scanning electron microscope (SEM, Zeiss Gemini Ultra-55). The elemental analysis was carried out using the energy dispersive spectroscopy (EDS) for both AgD/Cu and GO/AgD/Cu substrates. The SERS spectra were recorded with a Raman spectrometer (Horiba HR-800) with laser excitation at the wavelength of 532 nm. The excitation laser beam of the Raman spectrometer had a focused spot size of about 1 μm in diameter at the excitation plane by passing through a 50× objective lens. The effective excitation power of the laser source was kept at 0.5 mW.

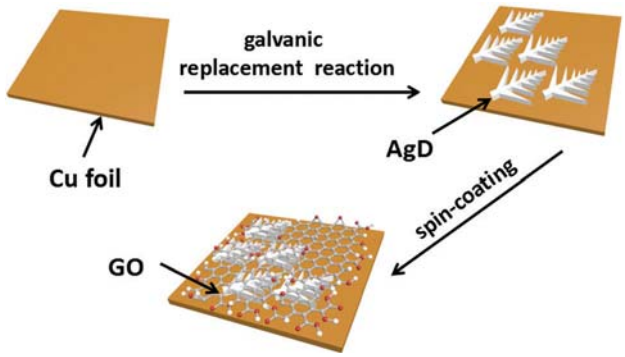

Fig. 1 Preparation processes of the GO/AgD/Cu substrate.

3. Results and discussion

The morphologies of the as-synthesized AgD and GO/AgD composite were observed by SEM. Fig. 2(a and b) show the typical SEM images of the as-synthesized AgD/Cu substrate. It can be clearly seen that AgD nanostructures that consist of one central stem with numerous side branches are formed by the galvanic replacement. The large-area and uniform AgD nanostructures can be grown on the Cu substrate, which can be confirmed *via* SEM images [see Fig. S1(a and b)] in the ESI.† Fig. 2(c) and (d) are the typical SEM images of the GO/AgD/Cu substrate. We can see that the observed morphologies of the GO-decorated AgD become blurred in contrast to the as-synthesized one, which is caused by the electron charging effect since the GO

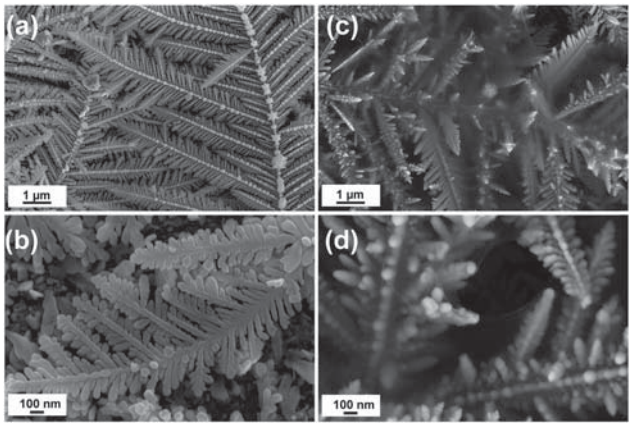

Fig. 2 Typical SEM images of the AgD/Cu substrate (a and b) and the GO/AgD/Cu substrate (c and d).

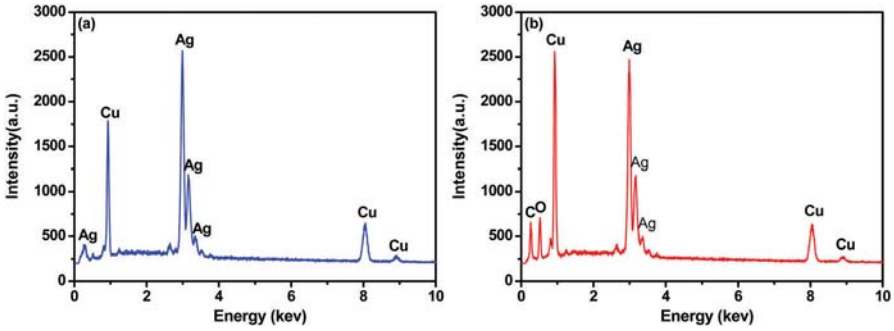

Fig. 3 EDS spectra of the AgD/Cu substrate (a) and the GO/AgD/Cu substrate (b).

has very poor electrical conductivity. This also indicates the coverage of GO on AgD. The GOs show a sheet-like shape, as shown in Fig. S1(c) (ESI†). From Fig. S1(c) (ESI†), with the increase of the number of the GO layers, the color becomes gradually dark. The GO layer is estimated to be ~50 nm from the cross-sectional SEM image of the GO/AgD/Cu substrate [see Fig. S1(d), ESI†]. From Fig. S1(d) (ESI†), we can see that the AgD layer shows a microscopically rough surface and the GO layer is almost conformally coated on the AgD/Cu substrate, indicating a reasonably uniform coating. The EDS spectra in Fig. 3 clearly show that there are additional C and O elements in the GO/AgD/Cu material compared to the as-synthesized AgD/Cu substrate, indicating the successful preparation of the GO/AgD/Cu substrate.

To further confirm the GO decoration, we carried out the Raman spectral measurement of the AgD/Cu and GO/AgD/Cu substrates, respectively, as shown in Fig. 4(a) and (b). In contrast, the GO/AgD/Cu substrate shows two obvious Raman peaks at ~1356 and ~1601 cm^{-1}, which correspond to the D and G bands of GO that are related to the vibrations of sp^3 and sp^2 carbon atoms of the disordered GO, respectively.[54,55] This observation further confirms the successful decoration of GO on AgD.

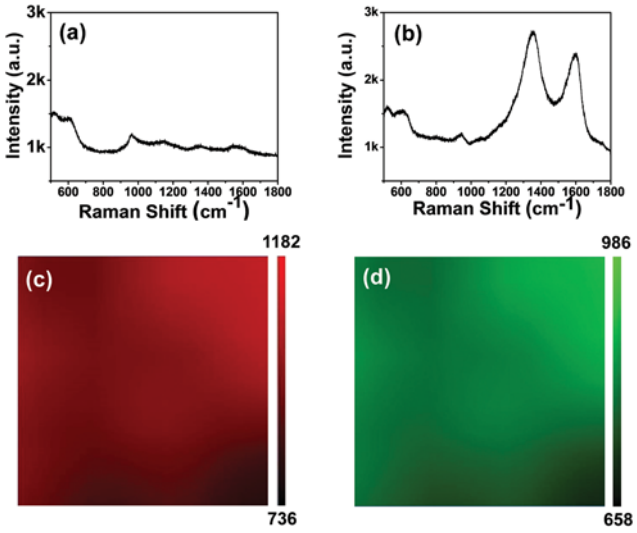

Fig. 4 Measured Raman spectra of the (a) AgD/Cu and (b) GO/AgD/Cu substrates. Raman mapping of (c) 1356 and (d) 1601 cm^{-1} peaks of GO on the GO/AgD/Cu substrate were implemented over an area of 20 × 20 μm^2.

Fig. 4(c) and (d) show Raman mapping of 1356 and 1601 cm^{-1} peaks of GO over an area of 20 × 20 μm^2 on the GO/AgD/Cu substrate. A relatively uniform color mapping can be observed at both peaks, indicating an even distribution of GO on the GO/AgD/Cu substrate.

Rhodamine 6G (R6G) was used as the probe molecule to evaluate the SERS performance of the GO/AgD/Cu substrate. For comparison, Raman spectra of R6G molecules absorbed on the AgD/Cu substrates before and after GO decoration were recorded, and the typical results are presented in Fig. 5. Fig. 5(a) shows the SERS spectra of R6G molecules from the AgD/Cu substrate with various concentrations of 10^{-6}, 10^{-7}, 10^{-8}, 10^{-9}, and 10^{-10} M, respectively. The observed Raman peaks at 612, 773, 1183, 1311, 1365, 1510 and 1650 cm^{-1} are in good agreement with previous reports for R6G.[55–57] In order to facilitate comparison and observation, these Raman spectra have been smoothed. Fig. 5(b) shows the Raman spectra of R6G molecules from the GO/AgD/Cu substrate with different concentrations, which exhibits clearly that the GO/Ag/Cu substrate is superior to the AgD/Cu substrate in terms of the enhancement effect. We can see that for the GO/Ag/Cu substrate, the characteristic signals of R6G are still distinguishable at the concentration of 10^{-11} M, which is one order of magnitude lower than that for the AgD/Cu one. This detection sensitivity is also higher than many other reported ones of the AgD-based composites.[28,58] Fig. 5(c) shows the relationship between Raman intensity and concentrations for both AgD/Cu and GO/AgD/Cu substrates at the selected peak of 612 cm^{-1}. Both substrates show an excellent linear response, indicating that they could be further utilized to quantitatively calculate the concentration of the detection analyte using SERS. Comparatively, the GO/AgD/Cu substrate shows slightly better linear response than the AgD/Cu one, which could be mainly attributed to the reduced border effect due to the existence of GO, making the R6G molecules absorbed on the surface more evenly. From Fig. 5(c), we also note that the AgD/Cu and GO/AgD/Cu substrates demonstrate slightly different slopes. The slope indicates the sensitivity of the SERS substrate. For the AgD/Cu substrate, the sensitivity is mainly determined by the number of "hot spots" that are produced by excitation of surface plasmons, referring to the electromagnetic enhancement. While for the GO/AgD/Cu substrate, the sensitivity is rather determined by a combination of chemical enhancement of GO and the number of "hot spots" of AgD. It has been known that electromagnetic

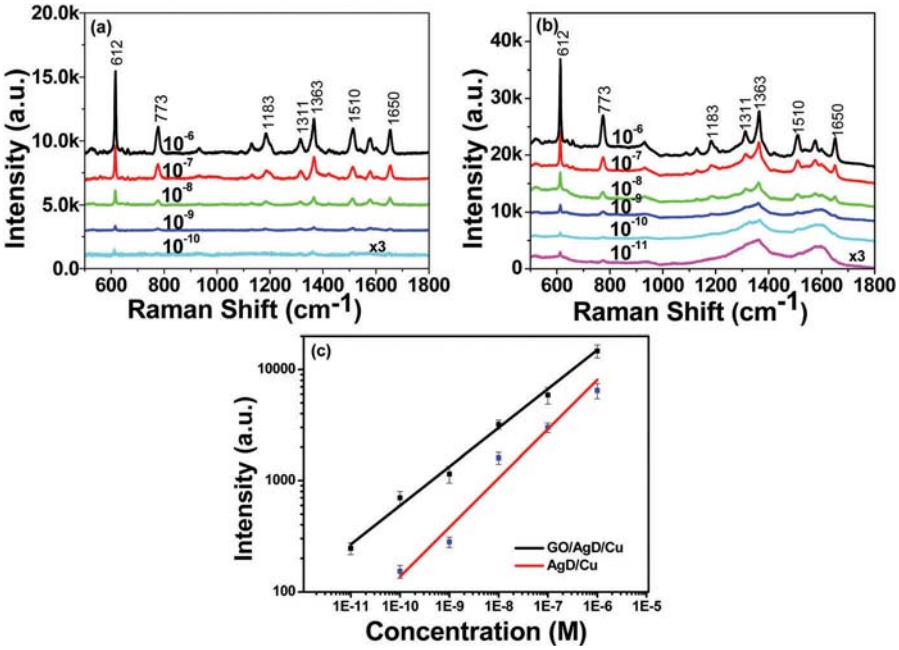

Fig. 5 Measured Raman spectra of R6G molecules on the (a) AgD/Cu and (b) GO/AgD/Cu substrate with different concentrations. (c) The corresponding plots of Raman intensity as a function of concentration at 612 cm^{-1}.

enhancement plays a dominant role (with a significant difference of multiple orders of magnitude on the enhancement) compared to the chemical one.[59] In our case, although the addition of the GO layer provides an additional enhancement, the addition of the GO layer also decreases the interaction between molecules and "hot spots". As a result, the slope slightly decreases with the addition of the GO layer.

Fig. 6 shows the raw Raman spectra of R6G with a concentration of 10^{-8} M adsorbed on the AgD/Cu and GO/AgD/Cu substrates, respectively. Obviously, the signal-to-noise ratio is significantly improved and the fluorescence background is greatly suppressed in the SERS spectra for the GO/AgD/Cu substrate. The addition of the graphene oxide layer isolates the R6G molecules from AgD and the spurious SERS signals from various possible metal–molecule interactions can therefore be suppressed. More importantly, the signal intensity from the GO/AgD/Cu substrate is remarkably increased compared to the AgD/Cu one. As a comparison, the SERS signals from the GO/AgD/Cu substrate at 612 cm^{-1} and 773 cm^{-1} are 2.4 times and 2.7 times stronger than that from the AgD/Cu one, respectively. To quantify the enhancement contribution from GO, we calculated the enhancement factor (EF) based on the following formula:[60]

$$\mathrm{EF} = \frac{I_{\mathrm{SERS}}/N_{\mathrm{SERS}}}{I_{\mathrm{RS}}/N_{\mathrm{RS}}}$$

where I_{SERS} and I_{RS} are the intensities of the same band, and N_{SERS} and N_{RS} are the numbers of R6G molecules illuminated by the laser spot under SERS and the normal Raman condition, respectively. According to the above formula, the average EF is calculated to be 7.2×10^6 for the AgD/Cu substrate. Similarly, the EF for the GO/AgD/Cu substrate is calculated to be 1.6×10^7. As a result, the EF for the GO/AgD/Cu substrate shows a 2.2-fold enhancement compared to the AgD/Cu one. We believe that this additional SERS enhancement results from two major factors. One factor is the chemical enhancement caused by the GO layer. Chemical enhancement is a short-range effect that requires the molecule to be in contact with or in close proximity to the substrate to allow charge transfer between the molecules and the substrate. The chemical enhancement of GOs arises from π–π stacking and charge transfer from the lone-pairs of electrons on the oxygen-containing functional groups of GOs to the probe molecules.[61–63] The other factor is the large surface-to-volume ratio induced by the Ag dendritic nanostructures. This further helps increase the GO–molecule interaction area and physical adsorption upon the addition of the GO layer. As a result, these two effects contribute collectively to the observed additional SERS enhancement.

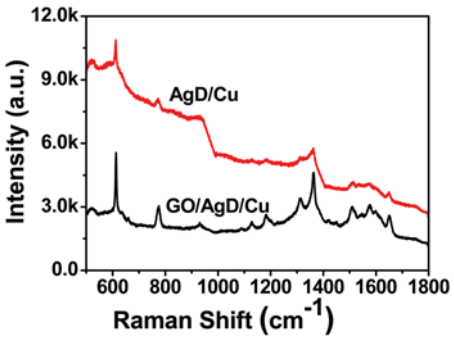

Fig. 6 Measured Raman spectra of R6G with a concentration of 10^{-8} M adsorbed on the AgD/Cu and GO/AgD/Cu substrates.

For SERS applications, in addition to high sensitivity, reproducibility and stability are usually another major concern.

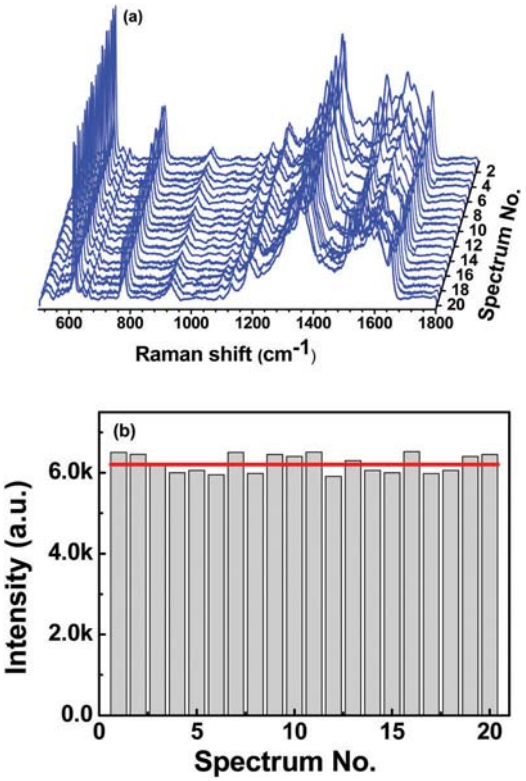

Fig. 7 (a) Measured SERS spectra of R6G molecules with the concentration of 10^{-7} M at 20 different positions on the GO/AgD/Cu substrate. (b) Spot-to-spot intensity variation of the characteristic peak at 612 cm^{-1} for the GO/AgD/Cu substrate.

For the reproducibility test, we carried out the collection of the SERS signals from randomly selected positions spacing larger than 2 mm for evaluation. Fig. 7(a) shows the measured SERS spectra of R6G molecules with the concentration of 10^{-7} M at 20 different positions on the GO/AgD/Cu substrate. The observed spectral profiles of Raman bands from different positions are very similar. There is neither an obvious shift of the major Raman peaks nor a significant change of the Raman intensity, indicating that the GO/AgD/Cu substrates are highly reproducible. The spot-to-spot intensity variation of the characteristic peak at 612 cm^{-1} for the GO/AgD/Cu substrate can be further quantitatively analyzed, as shown in Fig. 7(b). The red line represents the averaged intensity of 20 spectra and the green zone represents ±5% intensity variation. The intensity deviation of the SERS spectra with respect to the average intensity is given by the formula:

$$D = \frac{\Delta I}{\bar{I}} \times 100\% = \frac{|I - \bar{I}|}{\bar{I}} \times 100\%$$

where D represents the intensity deviation of the characteristic 612 cm^{-1} peak at the GO/AgD/Cu substrate, I is the peak intensity and $\bar{I}$ is the average peak intensity. Calculations for the 20 data points show that the intensity deviation is less than 6%, further confirming the high reproducibility of the GO/AgD/Cu substrate. This proves that although the AgD layer on the Cu substrate shows a microscopically rough surface [see Fig. S1(d), ESI†], it does not affect the SERS performance macroscopically, hence making the GO/AgD/Cu substrates highly promising for reproducible, cost-effective SERS applications.

In our design, in addition to the SERS enhancement, we also expect the GO decoration to serve as a protective layer that prevents the Ag dendrites from oxidation. The long-term stability of the GO/AgD/Cu substrate was therefore examined. Fig. 8(a) and (b) show the SERS spectra of R6G with the concentration of 10^{-7} M absorbed on the as-synthesized AgD/Cu and GO/AgD/Cu substrates by exposing them to the ambient air environment for 0 day and 20 days, respectively. For the GO/AgD/Cu substrate, the characteristic peak intensity at 612 cm^{-1} decreases from 11 681 to 10 935, *i.e.* 6%, after 20 days, which is still in the position-dependent variation range of 6%. We can therefore conclude that there is no significant change in the SERS intensity for the GO/AgD/Cu substrate, demonstrating excellent stability. In contrast, the SERS signal intensity at the same spectral position has a drastic drop for the AgD/Cu substrate, which is decreased from 4128 to 2885, *i.e.* 30%, which is far beyond the variation range. This comparison confirms that GO decoration has greatly enhanced long term stability due to its outstanding and unique chemical properties. To further confirm the protection role of the GO layer, we further carried out the XPS test for the prepared substrates, as shown in Fig. S2(a–c) in the ESI.† Fig. S2(a and b) (ESI†) shows the XPS results for one AgD/Cu substrate exposed to the ambient air environment for 7 and 30 days, respectively. The respective atom ratios of Ag and O are estimated to be 87.74% and 65.26%, indicating that AgD has been further oxidized after long-time

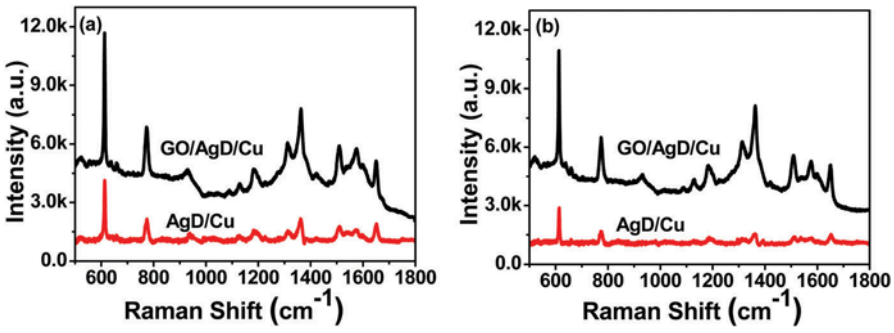

Fig. 8 Measured SERS spectra of R6G with the concentration of 10^{-7} M absorbed on the as-synthesized AgD/Cu and GO/AgD/Cu substrates by exposing them for (a) 0 day and (b) 20 days.

exposure. Fig. S2(c) (ESI†) shows the XPS result for a GO/AgD/Cu substrate. We can see that the signal for Ag at the GO-coated substrate is quite weak. This is due to the addition of the GO layer, which limits the detection depth of XPS. As a result, it is difficult to directly compare and analyze the Ag to O ratio in such a case and achieve the information about the Ag oxidation. However, we could induce the information of Ag oxidation by comparing the stabilities of SERS signals from AgD/Cu and GO/AgD/Cu substrates. Fig. S2(d) (ESI†) shows the comparison result of the AgD/Cu and GO/AgD/Cu substrates that are exposed to the ambient air environment for 0, 7, 14, 21, and 28 days. It can be clearly seen that the GO/AgD/Cu substrate has demonstrated much better stability than the AgD/Cu one, indicating that the GO layer indeed helps protect the AgD layer from oxidation.

4. Conclusion

We have demonstrated an excellent GO/AgD/Cu SERS substrate based on a facile and low-cost method. It has a minimum detection concentration of R6G as low as 10^{-11} M, which is one order of magnitude lower than the AgD/Cu substrate. Our experimental results showed that the decorated GO layer not only helps further enhance the SERS performance, but also protects Ag dendritic nanostructures from oxidation. The GO/AgD/Cu substrate possessed superior SERS performance in terms of sensitivity, uniformity, signal-to-noise ratio and stability. These advantageous features make the GO/AgD/Cu substrates highly promising for analytical purposes in SERS applications.

Acknowledgements

This work was supported by the National Natural Science Foundation of China (NSFC) (11674199) and the Excellent Young Scholars Research Fund of Shandong Normal University.

References

1 P. L. Stiles, J. A. Dieringer, N. C. Shah and R. P. Van Duyne, Surface-enhanced Raman spectroscopy, *Annu. Rev. Anal. Chem.*, 2008, **1**, 601–626.
2 B. Sharma, R. R. Frontiera, A.-I. Henry, E. Ringe and R. P. Van Duyne, SERS: materials, applications, and the future, *Mater. Today*, 2012, **15**, 16–25.
3 Y. S. Huh, A. J. Chung and D. Erickson, Surface enhanced Raman spectroscopy and its application to molecular and cellular analysis, *Microfluid. Nanofluid.*, 2009, **6**, 285–297.
4 B. Yan, A. Thubagere, W. R. Premasiri, L. D. Ziegler, L. Dal Negro and B. M. Reinhard, Engineered SERS substrates with multiscale signal enhancement: nanoparticle cluster arrays, *ACS Nano*, 2009, **3**, 1190–1202.
5 K. Xu, C. Zhang, R. Zhou, R. Ji and M. Hong, Hybrid micro/nano-structure formation by angular laser texturing of Si surface for surface enhanced Raman scattering, *Opt. Express*, 2016, **24**, 10352–10358.
6 A. Lagarkov, I. Budashov, V. Chistyaev, A. Ezhov, A. Fedyanin, A. Ivanov, I. Kurochkin, S. Kosolobov, A. Latyshev, D. Nasimov, I. Ryzhikov, M. Shcherbakov, A. Vaskin and A. K. Sarychev, SERS-active dielectric metamaterials based on periodic nanostructures, *Opt. Express*, 2016, **24**, 7133–7150.
7 Y.-L. Deng and Y.-J. Juang, Black silicon SERS substrate: Effect of surface morphology on SERS detection and application of single algal cell analysis, *Biosens. Bioelectron.*, 2014, **53**, 37–42.
8 X. Yang, H. Zhong, Y. Zhu, J. Shen and C. Li, Ultrasensitive and recyclable SERS substrate based on Au-decorated Si nanowire arrays, *Dalton Trans.*, 2013, **42**, 14324–14330.
9 G. Sinha, L. E. Depero and I. Alessandri, Recyclable SERS substrates based on Au-coated ZnO nanorods, *ACS Appl. Mater. Interfaces*, 2011, **3**, 2557–2563.
10 K. A. Willets and R. P. Van Duyne, Localized surface plasmon resonance spectroscopy and sensing, *Annu. Rev. Phys. Chem.*, 2007, **58**, 267–297.
11 S. J. Lee, A. R. Morrill and M. Moskovits, Hot spots in silver nanowire bundles for surface-enhanced Raman spectroscopy, *J. Am. Chem. Soc.*, 2006, **128**, 2200–2201.
12 H. K. Lee, Y. H. Lee, I. Y. Phang, J. Wei, Y.-E. Miao, T. Liu and X. Y. Ling, Plasmonic liquid marbles: A miniature substrate-less SERS platform for quantitative and multiplex ultratrace molecular detection, *Angew. Chem.*, 2014, **126**, 5154–5158.
13 G. Sinha, L. E. Depero and I. Alessandri, Recyclable SERS substrates based on Au-coated ZnO nanorods, *ACS Appl. Mater. Interfaces*, 2011, **3**, 2557–2563.
14 F. L. Yap, P. Thoniyot, S. Krishnan and S. Krishnamoorthy, Nanoparticle cluster arrays for high-performance SERS through directed self-assembly on flat substrates and on optical fibers, *ACS Nano*, 2012, **6**, 2056–2070.
15 B. Sharma, M. F. Cardinal, S. L. Kleinman, N. G. Greeneltch, R. R. Frontiera, M. G. Blaber, G. C. Schatz and R. P. Van Duyne, High performance SERS substrates: advances and challenges, *MRS Bull.*, 2013, **38**, 615–624.
16 Q. Zhang, Y. H. Lee, I. Y. Phang, C. K. Lee and X. Y. Ling, Hierarchical 3D SERS substrates fabricated by integrating photolithographic microstructures and self-assembly of silver nanoparticles, *Small*, 2014, **10**, 2703–2711.
17 P. He, H. Liu, Z. Li, Y. Liu, X. Xu and J. Li, Electrochemical deposition of silver in room-temperature ionic liquids and its surface-enhanced Raman scattering effect, *Langmuir*, 2004, **20**, 10260–10267.
18 Z. Yuan, N. H. Dryden, J. J. Vittal and R. J. Puddephatt, Chemical vapor deposition of silver, *Chem. Mater.*, 1995, **7**, 1696–1702.
19 J. C. Hulteen, D. A. Treichel, M. T. Smith, M. L. Duval, T. R. Jensen and R. P. Van Duyne, Nanosphere lithography: size-tunable silver nanoparticle and surface cluster arrays, *J. Phys. Chem. B*, 1999, **103**, 3854–3863.
20 N. Leopold and B. Lendl, A new method for fast preparation of highly surface-enhanced Raman scattering (SERS) active silver colloids at room temperature by reduction of silver nitrate with hydroxylamine hydrochloride, *J. Phys. Chem. B*, 2003, **107**, 5723–5727.

21 Y. Wang, B. Yan and L. Chen, SERS tags: novel optical nanoprobes for bioanalysis, *Chem. Rev.*, 2013, **113**, 1391–1428.
22 J. M. McLellan, Z.-Y. Li, A. R. Siekkinen and Y. Xia, The SERS activity of a supported Ag nanocube strongly depends on its orientation relative to laser polarization, *Nano Lett.*, 2007, **7**, 1013–1017.
23 S. Yang, D. Slotcavage, J. D. Mai, F. Guo, S. Li, Y. Zhao, Y. Lei, C. E. Cameron and T. J. Huang, Electrochemically created highly surface roughened Ag nanoplate arrays for SERS biosensing applications, *J. Mater. Chem. C*, 2014, **2**, 8350–8356.
24 M. Li, Y. Zhao, M. Cui, C. Wang and Q. Song, SERS-active Ag nanostars substrates for sensitive detection of ethyl carbamate in wine, *Anal. Sci.*, 2016, **32**, 725–728.
25 S. Wang, L. P. Xu, Y. Wen, H. Du, S. Wang and X. Zhang, Space-confined fabrication of silver nanodendrites and their enhanced SERS activity, *Nanoscale*, 2013, **5**, 4284–4290.
26 L. Fu, T. Tamanna, W.-J. Hu and A. Yu, Chemical preparation and applications of silver dendrites, *Chem. Pap.*, 2014, **68**, 1283–1297.
27 L. Hu, Y. J. Liu, S. Xu, Z. Li, J. Guo, S. Gao, Z. Lu, H. Si, S. Jiang and S. Wang, Facile and low-cost fabrication of Ag–Cu substrates *via* replacement reaction for highly sensitive SERS applications, *Chem. Phys. Lett.*, 2017, **667**, 351–356.
28 Y. F. Chan, C. X. Zhang, Z. L. Wu, D. M. Zhao, W. Wang, H. J. Xu and X. M. Sun, Ag dendritic nanostructures as ultrastable substrates for surface-enhanced Raman scattering, *Appl. Phys. Lett.*, 2013, **102**, 183118.
29 Q. X. Zhang, Y. X. Chen, Z. Guo, H. L. Liu, D. P. Wang and X. J. Huang, Bioinspired multifunctional hetero-hierarchical micro/nanostructure tetragonal array with self-cleaning, anticorrosion, and concentrators for the SERS detection, *ACS Appl. Mater. Interfaces*, 2013, **5**, 10633–10642.
30 S. Xie, X. Zhang, D. Xiao, M. C. Paau, J. Huang and M. M. F. Choi, Fast growth synthesis of silver dendrite crystals assisted by sulfate ion and its application for surface-enhanced Raman scattering, *J. Phys. Chem. C*, 2011, **115**, 9943–9951.
31 T. You, O. Niwa, M. Tomita and S. Hirono, Characterization of platinum nanoparticle-embedded carbon film electrode and its detection of hydrogen peroxide, *Anal. Chem.*, 2003, **75**, 2080–2085.
32 L. Fu, G. Lai, B. Jia and A. Yu, Preparation and electrocatalytic properties of polydopamine functionalized reduced graphene oxide–silver nanocomposites, *Electrocatalysis*, 2015, **6**, 72–76.
33 J. Huang, S. Vongehr, S. Tang, H. Lu, J. Shen and X. Meng, Ag dendrite-based Au/Ag bimetallic nanostructures with strongly enhanced catalytic activity, *Langmuir*, 2009, **25**, 11890–11896.
34 X. Zhang, F. Shi, J. Niu, Y. Jiang and Z. Wang, Superhydrophobic surfaces: from structural control to functional application, *J. Mater. Chem.*, 2008, **18**, 621–633.
35 S. Abalde-Cela, P. Aldeanueva-Potel, C. Mateo-Mateo, L. Rodriguez-Lorenzo, R. A. Alvarez-Puebla and L. M. Liz-Marzan, Surface-enhanced Raman scattering biomedical applications of plasmonic colloidal particles, *J. R. Soc., Interface*, 2010, **7**, S435–S450.
36 A. K. Geim and K. S. Novoselov, The rise of graphene, *Nat. Mater.*, 2007, **6**, 183–191.
37 X. Ling and J. Zhang, Interference phenomenon in graphene enhanced Raman scattering, *J. Phys. Chem. C*, 2011, **115**, 2835–2840.
38 C. Zhang, S. Z. Jiang, Y. Y. Huo, A. H. Liu, S. C. Xu, X. Y. Liu, Z. C. Sun, Y. Y. Xu, Z. Li and B. Y. Man, SERS detection of R6G based on a novel graphene oxide/silver nanoparticles/silicon pyramid arrays structure, *Opt. Express*, 2015, **23**, 24811–24821.
39 G. Goncalves, P. Marques, C. M. Granadeiro, H. I. S. Nogueira, M. K. Singh and J. Grácio, Surface modification of graphene nanosheets with gold nanoparticles: the role of oxygen moieties at graphene surface on gold nucleation and growth, *Chem. Mater.*, 2009, **21**, 4796–4802.
40 H. Chi, Y. J. Liu, F. Wang and C. He, Highly sensitive and fast response colorimetric humidity sensors based on graphene oxide film, *ACS Appl. Mater. Interfaces*, 2015, **7**, 19882–19886.
41 W. Ren, Y. Fang and E. Wang, A binary functional substrate for enrichment and ultrasensitive SERS spectroscopic detection of folic acid using graphene oxide/Ag nanoparticle hybrids, *ACS Nano*, 2011, **5**, 6425–6433.
42 A. Saha, S. Palmal and N. R. Jana, Highly reproducible and sensitive surface-enhanced Raman scattering from colloidal plasmonic nanoparticle *via* stabilization of hot spots in graphene oxide liquid crystal, *Nanoscale*, 2012, **4**, 6649–6657.
43 W. Fan, Y. H. Lee, S. Pedireddy, Q. Zhang, T. Liu and X. Y. Ling, Graphene oxide and shape-controlled silver nanoparticle hybrids for ultrasensitive single-particle surface-enhanced Raman scattering (SERS) sensing, *Nanoscale*, 2014, **6**, 4843–4851.
44 X. Wang, G. Meng, C. Zhu, Z. Huang, Y. Qian, K. Sun and X. Zhu, A generic synthetic approach to large-scale pristine-graphene/metal-nanoparticles hybrids, *Adv. Funct. Mater.*, 2013, **23**, 5771–5777.
45 X. Liu, L. Cao, W. Song, K. Ai and L. Lu, Functionalizing metal nanostructured film with graphene oxide for ultrasensitive detection of aromatic molecules by surface-enhanced Raman spectroscopy, *ACS Appl. Mater. Interfaces*, 2011, **3**, 2944–2952.
46 G. Lu, H. Li, C. Liusman, Z. Yin, S. Wu and H. Zhang, Surface enhanced Raman scattering of Ag or Au nanoparticle-decorated reduced graphene oxide for detection of aromatic molecules, *Chem. Sci.*, 2011, **2**, 1817–1821.
47 C. Hu, Y. Liu, J. Qin, G. Nie, B. Lei, Y. Xiao, M. Zheng and J. Rong, Fabrication of reduced graphene oxide and sliver nanoparticle hybrids for Raman detection of absorbed folic acid: a potential cancer diagnostic probe, *ACS Appl. Mater. Interfaces*, 2013, **5**, 4760–4768.
48 S. Murphy, L. Huang and P. V. Kamat, Synergetic effects of reduced graphene oxide and silver nanoparticles in SERS enhancement, *J. Phys. Chem. C*, 2013, **117**, 4740–4747.
49 L. Zhang, C. Jiang and Z. Zhang, Graphene oxide embedded sandwich nanostructures for enhanced Raman readout and

their applications in pesticide monitoring, *Nanoscale*, 2013, **5**, 3773–3779.

50 X. Li, W. C. H. Choy, X. Ren, D. Zhang and H. Lu, Highly intensified surface enhanced Raman scattering by using monolayer graphene as the nanospacer of metal film–metal nanoparticle coupling system, *Adv. Funct. Mater.*, 2014, **24**, 3114–3122.

51 P. Wang, O. Liang, W. Zhang, T. Schroeder and Y.-H. Xie, Ultra-sensitive graphene-plasmonic hybrid platform for label-free detection, *Adv. Mater.*, 2013, **25**, 4918–4924.

52 M. Losurdo, I. Bergmair, B. Dastmalchi, T.-H. Kim, M. M. Giangregroio, W. Jiao, G. V. Bianco, A. S. Brown, K. Hingerl and G. Bruno, Graphene as an electron shuttle for silver deoxidation: removing a key barrier to plasmonics and metamaterials for SERS in the visible, *Adv. Funct. Mater.*, 2014, **24**, 1864–1878.

53 Z.-L. Song, Z. Chen, X. Bian, L.-Y. Zhou, D. Ding, H. Liang, Y.-X. Zou, S.-S. Wang, L. Chen, C. Yang, X.-B. Zhang and W. Tan, Alkyne-functionalized superstable graphitic silver nanoparticles for Raman imaging, *J. Am. Chem. Soc.*, 2014, **136**, 13558–13561.

54 H. Wang, D. Sun, N. Zhao, X. Yang, Y. Shi, J. Li, Z. Su and G. Wei, Thermo-sensitive graphene oxide–polymer nanoparticle hybrids: synthesis, characterization, biocompatibility and drug delivery, *J. Mater. Chem. B*, 2014, **2**, 1362–1370.

55 Z. Liu, Y. Wang, R. Deng, L. Yang, S. Yu, S. Xu and W. Xu, Fe_3O_4@Graphene Oxide@Ag particles for surface magnet solid-phase extraction surface-enhanced Raman scattering (SMSPE-SERS): from sample pretreatment to detection all-in-one, *ACS Appl. Mater. Interfaces*, 2016, **8**, 14160–14168.

56 G. Li, H. Li, Y. Mo, X. Huang and L. Chen, Surface enhanced resonance Raman spectroscopy of rhodamine 6G adsorbed on silver electrode in lithium batteries, *Chem. Phys. Lett.*, 2000, **330**, 249–254.

57 Y. K. Kim, S. W. Han and D. H. Min, Graphene oxide sheath on Ag nanoparticle/graphene hybrid films as an antioxidative coating and enhancer of surface-enhanced Raman scattering, *ACS Appl. Mater. Interfaces*, 2012, **4**, 6545–6551.

58 L. Fu, D. Zhu and A. Yu, Galvanic replacement synthesis of silver dendrites-reduced graphene oxide composites and their surface-enhanced Raman scattering characteristics, *Spectrochim. Acta, Part A*, 2015, **149**, 396–401.

59 W. Xu, X. Ling, J. Xiao, M. S. Dresselhaus, J. Kong, H. Xu, Z. Liu and J. Zhang, Surface enhanced Raman spectroscopy on a flat graphene surface, *Proc. Natl. Acad. Sci. U. S. A.*, 2012, **109**, 9281–9286.

60 E. C. Le Ru, E. Blackie, M. Meyer and P. G. Etchegoin, Surface enhanced Raman scattering enhancement factors: a comprehensive study, *J. Phys. Chem. C*, 2007, **111**, 13794–13803.

61 X. Yu, H. Cai, W. Zhang, X. Li, N. Pan, Y. Luo, X. Wang and J. G. Hou, Tuning chemical enhancement of SERS by controlling the chemical reduction of graphene oxide nanosheets, *ACS Nano*, 2011, **5**, 952–958.

62 X. Liu, L. Cao, W. Song, K. Ai and L. Lu, Functionalizing metal nanostructured film with graphene oxide for ultrasensitive detection of aromatic molecules by surface-enhanced Raman spectroscopy, *ACS Appl. Mater. Interfaces*, 2011, **3**, 2944–2952.

63 W. Fan, Y. H. Lee, S. Pedireddy, Q. Zhang, T. Liu and X. Y. Ling, Graphene oxide and shape-controlled silver nanoparticle hybrids for ultrasensitive single-particle surface-enhanced Raman scattering (SERS) sensing, *Nanoscale*, 2014, **6**, 4843–4851.